Nonlinear Dyn (2019) 98:1821–1830
https://doi.org/10.1007/s11071-019-05290-1

ORIGINAL PAPER

Ratcheting based on neighboring niches determines lifestyle

Ye Ye · Xiao Rong Hang · Jin Ming Koh · Jarosław Adam Miszczak · Kang Hao Cheong · Neng Gang Xie

Received: 28 February 2019 / Accepted: 4 October 2019 / Published online: 9 November 2019
© Springer Nature B.V. 2019

Abstract In this paper, a co-evolution method of game dynamics and network structure is adopted to demonstrate that neighboring niches of an individual or population may have great influence in determining lifestyle adoption. The model encompasses network structure evolution, denoted **Case A**, and pure games participated in by individuals in the network with two asymmetric branches determining winning and losing states, denoted **Case B**. The selection between game branches is dependent on the demographic of neighboring niches, and favorable or unfavorable effects from the neighborhood can be made to manifest by setting probabilistic game parameters. Theoretical analysis reveals that losing configurations of **Case B**, when stochastically mixed with neutral **Case A**, can result in paradoxical winning scenarios where the network experiences positive gain—a Parrondo's paradox-like phenomenon has therefore emerged. It is elucidated that agitation from **Case A** increases the probability of individuals to play the favorable branch of **Case B**, leading to unexpected gains in two distinct parameter regimes. In the paradoxical regions, our analysis suggests strongly that neighboring niches are the cause for evolution toward social or solitary lifestyle behaviors, and we present important connections to real-world biological life.

Keywords Population dynamics · Parrondo's paradox · Nonlinear dynamics · Ratcheting · Neighboring niches

Y. Ye
School of Mechanical Engineering, Anhui University of Technology, Ma'anshan 243002, Anhui, China

X. R. Hang · N. G. Xie (✉)
School of Management Science and Engineering, Anhui University of Technology, Ma'anshan 243002, Anhui, China
e-mail: xienenggang@aliyun.com

J. M. Koh · K. H. Cheong (✉)
Science and Math Cluster, Singapore University of Technology and Design, 8 Somapah Road, Singapore 487372, Singapore
e-mail: kanghao_cheong@sutd.edu.sg

J. A. Miszczak
Institute of Theoretical and Applied Informatics, Polish Academy of Sciences, Ba ltycka 5, 44-100 Gliwice, Poland

1 Introduction

Many phenomena in nature and human society indicate that an individual's living behavior depends on the niches of his neighbors. For social organisms, due to cooperative behavioral adaptations in foraging and group defense mechanisms in facing external invasion, a good neighboring niche positively promotes individual survival fitness. For solitary organisms, because of food scarcity and reproductive competition, strong neighbors can yield great competitive pressure on their survival. Whether they live in cooperative colonies or in solitude, that the lineages of life had thus far persisted indicates a degree of adaptability—and this raises a question of the mechanism responsible for the evolu-

tion of different lifestyle behaviors. What factors affect these evolutionary paths, and what roles do adjacent populations play in influencing evolutionary dynamics?

In investigating the influence of neighboring niches on individual survival, John Conway [1] invented the *Game of Life*. In this game, a group of cells is assumed to be living in a two-dimensional square lattice grid. Each cell occupies a grid (an unoccupied grid is called a blank space). The states of eight neighboring cells—four adjacent orthogonally and four adjacent diagonally—constitute neighboring niches. The game rules define birth, death and survival processes, in that (1) if an empty grid has 3 neighboring cells, a new cell is birthed and placed into it at the next time step, (2) if a cell has 4 or more neighboring cells, it will die from overpopulation, and if a cell does not have more than 1 neighboring cell, it will die from isolation, and (3) if a cell has 2 or 3 neighboring cells, it will continue to exist. Simulation results reveal intriguing patterns, reflecting somewhat unexpectedly that complex phenomena can be derived from simplistic, almost trivial, rules. The *Game of Life* is one of the simplest and most famous cellular automaton systems within the scientific community. Based on this model, various studies have mimicked diverse aspects of complexity in nature [2–8], and cellular automata have also seen applications in digital image processing and encryption [9–11].

In [12], Toral had introduced a multi-agent Parrondo's game, played with $N \geq 1$ players. The game structure constitutes distinct branches dependent on the winning and losing states of the neighbors of each player. For a one-dimensional line topology [13,14], the neighboring niches consist only of the two neighbors on both sides, and there are hence four branches. In [15], Mihailovic proposed a Parrondo's game with mechanics dependent on two-dimensional neighboring niches. Simulation results indicate that the neighboring niches have large effects on the winning or losing outcomes of individuals. For a population composed of N^2 individuals, each individual occupies a grid in a $N \times N$ two-dimensional lattice. Four orthogonally adjacent neighbors constitute neighboring niches. The game model was constructed as an analogue of the canonical Parrondo's paradox [16–24], consisting of a pair of distinct branches with different rules, labeled Game A and Game B. Game A is played by only one player on each round, and only one biased coin is flipped. Game B comprises five sub-branches selected based on the winning and losing states of neighboring individuals (for four neighbors, the number of winners $N_W \in \{0, 1, 2, 3, 4\}$), with corresponding winning probabilities p_i where $i \in \{0, 1, 2, 3, 4\}$, respectively. Simulations show that playing Game A or Game B individually is always losing, but if Game A and Game B are played randomly or in a certain deterministic sequence, a winning result can be generated. This unexpected occurrence of winning outcomes in a seemingly losing game is known as the *Parrondo's paradox*.

It is noted that all the above games focus on the modification of Game B. In [25], Toral proposed a modified multi-agent Game A. In this new game, capital transfer between two randomly selected players provides perturbative effects. On the basis of this model, Ye et al. [26] had designed a complementary Game A structure that reflects plausible competitive and cooperative relationships between individuals, and the effects of competitive and cooperative behaviors were explored through simulation analysis.

Conceivably, neighboring niches can have considerable impact on an individual, influencing payoffs in winning and losing outcomes, and strategic value and therefore adaptation toward competitive and cooperative behaviors. Is it possible, then, that influence from neighboring niches is the primary driving factor in evolution toward social and solitary lifestyles? In this paper, we develop a new game structure encompassing neighbor niche-dependent evolution on a lattice grid. In the proposed structure, branching is dependent on the number of winners and losers in the neighborhood, instead of distinct winning and losing states. A lattice network evolution over time is adopted. Through a theoretical analysis, we find that a ratcheting mechanism analogous to that in Parrondo's paradox drives the evolution of lifestyles, with heavy dependence on the configuration of neighboring niches.

2 Game rules

Environment. Our model utilizes a 3×3 two-dimensional lattice network. Each individual occupies a grid within this network, and four orthogonally adjacent neighbors constitute the neighboring niches. An example of such a network, consisting nine individuals, is illustrated in Fig. 1a. We adopt periodic boundary conditions [15,27] such that the lattice is effectively closed into a sphere, thus ensuring that each individual has four orthogo-

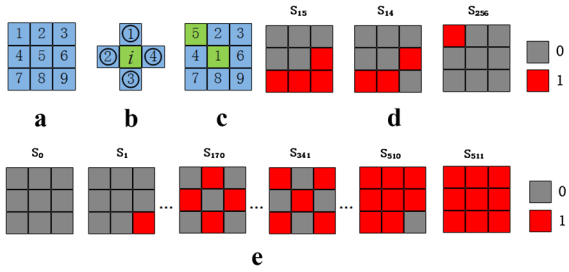

Fig. 1 Series of illustrations of the 3×3 lattice network considered. **a** Individuals numbered 1 through 9, each occupying a grid in the lattice. **b** The four orthogonally adjacent neighbors to an individual and their labels. **c** The network lattice after the swapping of individuals 1 and 5 under the specified evolution rules. **d** Illustration of various ensemble states, where individuals colored gray are in a losing state, denoted 0, and individuals colored red are in a winning state, denoted 1

nally adjacent neighbors regardless of position in the network. These four neighbors are labeled ①, ②, ③ and ④ in the order of up, left, bottom, and right, respectively, as shown in Fig. 1b. Taking individual 1 located at the corner of the network (shown in Fig. 1a) for instance, the ①, ②, ③ and ④ neighbors correspond to individuals 7, 3, 4 and 2, respectively, due to the periodic boundary conditions.

Evolution rules. Lattice network evolution over time occurs under the premise that the network topology remains unchanged (a two-dimensional lattice is maintained). The adopted evolutionary mechanism is as follows: (1) at each time step, two individuals, individual i and individual j, are randomly selected from the 3×3 lattice, and (2) the locations of individual i and individual j are exchanged, with neighbor connections subsequently re-stablished between the swapped pair, subject to the periodic boundary conditions. As a demonstration, the lattice configuration after a swap of individuals 1 and 5 is shown in Fig. 1c, illustrating the mechanism. Prior neighbor connections are not carried over during the evolution process.

Pure games. Dependent on the winning and losing states of neighboring niches, the structure of the game is divided into two branches. If the number of winners in the neighborhood is less than the number of losers, Branch 1 is played with a winning probability p_1, else, if the number of winners in the neighborhood is not less than the number of losers, Branch 2 is played with a winning probability p_2. During a game round, an individual on the lattice is selected at random to participate and receives an outcome in accordance to these rules—in other words, the game process is asynchronous [13]. The individual receives a unit of capital for a win and loses a unit of capital for a loss.

Progression. At each time step, the network lattice may undergo evolution, or a player may be chosen to participate in pure games and receive an updated winning or losing state. Selection between these possible options is stochastic, with probability γ for evolution and $1 - \gamma$ for pure games.

3 Theoretical analysis

In this section, we describe an analytical approach to describe the dynamics of the lattice network under the stated game model. We first examine ensemble dynamics under evolution-only circumstances (denoted **Case A**), followed by evolution-free, pure-game only dynamics (denoted **Case B**). The combination of theoretical results from these two then enables the analysis of the full dynamics encompassing both network evolution and pure games (denoted **Case C**).

3.1 Evolution-only ensemble dynamics (Case A)

There is a total of $2^9 = 512$ possible winning/losing ensemble game states in the 3×3 lattice, as shown in Fig. 1e. We label these ensemble states in running decimal notation from S_0 to S_{511}, such that the state set $S = \{S_0, S_1, \ldots, S_{511}\}$. The transition probability matrix between states is then

$$\mathbf{P} = \left[p_{S_x \to S_y}\right]_{S_x, S_y \in S}. \tag{1}$$

Network evolution through the discussed swapping mechanism will change the location of individuals in the ensemble. In this way, the winning/losing states of the ensemble will be modified. In accordance with the specified evolution rules, there are $C_9^2 = 36$ distinct types of location changes (random selection of two individuals from a 3×3 lattice grid). After an evolution round, the ensemble state S_{t+1} at time $t + 1$ can either be the same as S_t at time t, or the game state may change—we examine these two cases in turn.

3.1.1 Unchanged game state ($S_{t+1} = S_t$)

Suppose there are d individuals in the losing state at time t in the ensemble. After an evolution round, if the ensemble state remains unchanged, only individuals with the same state can have exchanged positions. Therefore, the transition probability can be expressed $p_{S_t \to S_{t+1}} = \left(C_d^2 + C_{9-d}^2\right)/C_9^2$. Sample calculations on $p_{15\to 15}$, corresponding to $S_{t+1} = S_t = S_{15}$ as shown in Fig. 1e, are detailed in Appendix A for clarity.

3.1.2 Changed game state ($S_{t+1} \neq S_t$)

Suppose, likewise, that there are d individuals in the losing state at time t in the ensemble. After an evolution round, if the ensemble state has changed, only individuals in opposite states can have exchanged positions. There are therefore $C_d^1 C_{9-d}^1$ kinds of location change, and the possible outcomes corresponding to each location change are distinct. The transition probability is therefore $p_{S_t \to S_{t+1}} = 1/C_9^2 = 1/36$.

Through the presented approach, the transition probability matrix $\mathbf{P}^A$ of the ensemble can be obtained. In this matrix, off-diagonal elements are either 0 or 1/36. The stationary distribution $\boldsymbol{\pi}^A$ can then be obtained from $\boldsymbol{\pi}^A = \boldsymbol{\pi}^A \mathbf{P}^A$. As network evolution alone does not on average generate a winning or losing outcome (it is fair), the expected gain $E^A = 0$, and $\lambda_{kl}^A = \lambda_{kw}^A = 1/2$ for $k \in \{0, 1, \ldots, 511\}$.

3.2 Evolution-free ensemble dynamics (Case B)

As before, at each game round, the ensemble state S_{t+1} at time $t+1$ can either be the same as S_t at time t, or the game state may change—again, we examine these two cases in turn.

3.2.1 Unchanged game state ($S_{t+1} = S_t$)

Let s_i denote the state of individual i in the lattice network, where $s_i = 0$ represents a losing state and $s_i = 1$ represents a winning state. As individuals are randomly selected, the probability of any individual i being selected is 1/9. We also denote the states of the neighbors of individual i as $\eta_i = \left\{s_i^1, s_i^2, s_i^3, s_i^4\right\}$, where s_i^1, s_i^2, s_i^3 and s_i^4 represent the states of neighbors ①, ②, ③ and ④ of individual i, respectively. As described in Sect. 2, the game branch to be played by individual i and the probability of winning $p_{\eta_i} \in \{p_1, p_2\}$ is determined by the states of its neighbors. The transition probability $p_{S_t \to S_{t+1}}$ is then given by

$$p_{S_t \to S_{t+1}} = \frac{1}{9} \sum\nolimits_{i=1}^{9} p\left(i\right), \tag{2}$$

where $p\left(i\right)$ denotes the probability that individual i remains in state s_i, expressed as

$$p\left(i\right) = \begin{cases} 1 - p_{\eta_i} & s_i = 0 \\ p_{\eta_i} & s_i = 1. \end{cases} \tag{3}$$

Sample calculations on $p_{15\to 15}$, corresponding to $S_{t+1} = S_t = S_{15}$ as shown in Fig. 1e, are detailed in Appendix B.

3.2.2 Changed game state ($S_{t+1} \neq S_t$)

Without loss of generality, it is assumed that the change in game state is caused by a state change of individual i, selected with probability 1/9. Then, the transition probability $p_{s_i(t)\to s_i(t+1)}$ from state $s_i\left(t\right)$ at time t to state $s_i\left(t+1\right)$ at time $t+1$ is

$$p_{s_i(t)\to s_i(t+1)} = \overline{p}(i)/9, \tag{4}$$

where state $s_i\left(t\right)$ switches to $s_i\left(t+1\right)$ with probability $\bar{p}(i)$, expressed as

$$\overline{p}\left(i\right) = \begin{cases} p_{\eta_i} & s_i(t) = 0 \\ 1 - p_{\eta_i} & s_i(t) = 1. \end{cases} \tag{5}$$

A sample calculation for $p_{15\to 14}$, representing a transition from state S_{15} to S_{14} (illustrated in Fig. 1d), can be found in Appendix B. Through the presented approach for both $S_{t+1} = S_t$ and $S_{t+1} \neq S_t$, the transition probability matrix $\mathbf{P}^B$ for **Case B** can be obtained. The transition probability matrix $\mathbf{P}^B$ can then be substituted into the steady-state equation $\boldsymbol{\pi}^B = \boldsymbol{\pi}^B \mathbf{P}^B$ to obtain the stationary probability distribution $\boldsymbol{\pi}^B$. The expected gain is then

$$E^B = \boldsymbol{\pi}^B \left(\boldsymbol{\lambda}_{\text{win}}^B - \boldsymbol{\lambda}_{\text{lose}}^B\right), \tag{6}$$

where $\boldsymbol{\lambda}_{\text{win}}^B = \left[\lambda_{0w}^B\ \lambda_{1w}^B \cdots \lambda_{511w}\right]^T$ and $\boldsymbol{\lambda}_{\text{lose}}^B = \left[\lambda_{0l}^B\ \lambda_{1l}^B \cdots \lambda_{511l}\right]^T$ are the average probabilities of winning and losing, respectively, for each ensemble game state from S_0 to S_{511}, satisfying $\lambda_{kl}^B = 1 - \lambda_{kw}^B$ for $k \in \{0, 1, \ldots, 511\}$. The expression for λ_{kw}^B is

$$\lambda_{kw}^B = \frac{1}{9} \sum\nolimits_{i=1}^{9} p_{k\eta_i}, \tag{7}$$

where i is an index running over all individuals, $\eta_i = \left\{s_i^1, s_i^2, s_i^3, s_i^4\right\}$ represents the neighboring niches

of individual i, $p_{k\eta_i} \in \{p_1, p_2\}$ is the probability of winning that individual i has with neighboring niches η_i when the ensemble is in state S_k. Taking S_{15} as an example (shown in Fig. 1d), the neighboring niches of each individual are $\eta_1 = \eta_2 = \{1,0,0,0\}$, $\eta_3 = \{1,0,1,0\}$, $\eta_4 = \{0,1,1,0\}$, $\eta_5 = \{0,0,1,1\}$, $\eta_6 = \{0,0,1,0\}$, $\eta_7 = \eta_8 = \{0,1,0,1\}$, and $\eta_9 = \{1,1,0,1\}$. It can then be computed using Eq. (7) that $\lambda^B_{15w} = (3p_1 + 6p_2)/9$.

3.3 Combined ensemble dynamics (Case C)

It is assumed that network evolution and pure games are selected to occur at each time step with equal probability, that is, $\gamma = 1/2$. The transition probability matrix for the combined ensemble dynamics is then

$$\mathbf{P}^C = \left(\mathbf{P}^A + \mathbf{P}^B\right)/2. \tag{8}$$

The stationary distribution can then be obtained from $\boldsymbol{\pi}^C = \boldsymbol{\pi}^C \mathbf{P}^C$, and the expected gain is

$$E^C = \boldsymbol{\pi}^C \left(\boldsymbol{\lambda}^C_{\text{win}} - \boldsymbol{\lambda}^C_{\text{lose}}\right), \tag{9}$$

where $\boldsymbol{\lambda}^C_{\text{win}} = \left[\lambda^C_{0w}\ \lambda^C_{1w} \cdots \lambda^C_{511w}\right]^T$ and $\boldsymbol{\lambda}^C_{\text{lose}} = \left[\lambda^C_{0l}\ \lambda^C_{1l} \cdots \lambda^C_{511l}\right]^T$ are the average probabilities of winning and losing, respectively, for each ensemble game state from S_0 to S_{511}, satisfying $\lambda^C_{kw} = \left(\lambda^A_{kw} + \lambda^B_{kw}\right)/2$ and $\lambda^C_{kl} = \left(\lambda^A_{kl} + \lambda^B_{kl}\right)/2$ for $k \in \{0, 1, \ldots, 511\}$.

4 Results and discussion

Figure 2a shows expected gains for the evolution-only **Case A**, evolution-free pure-game **Case B** and the combined pure games-evolution **Case C**, and Fig. 2b presents a phase diagram across $p_1 - p_2$ parameter space, in which blue regions indicate where the conditions $E^C \geq E^B$ and $E^B < 0$ are satisfied, and red regions indicate where $E^C \geq 0$ and $E^B < 0$ are satisfied. As the expected gain for the evolution-only **Case A** is 0, the red regions indicate the occurrence of the Parrondo's paradox [19,20,28–32], in which a losing strategy (**Case B**) and a neutral strategy (**Case A**) combine to yield a winning one (**Case C**). Specifically, this is known as the weak Parrondo effect [33], in contrast to the strong effect wherein two losing strategies yield winning outcomes. We notice that the red regions are composed of two disconnected sub-regimes, one of which is the upper left space where p_1 is very small and p_2 very large, and the other of which is the lower right space, where p_1 is very large and p_2 is very small.

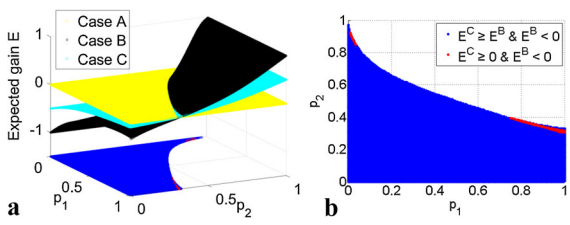

Fig. 2 Theoretical analysis results. **a** Expected gain E for **Case A**, **Case B**, and **Case C** across p_1–p_2 parameter space. **b** Phase diagram, red regions highlight paradoxical scenarios where a losing **Case B** and a fair **Case A** combine to yield a winning **Case C**. (Color figure online)

4.1 Analysis of paradoxical mechanism

To further examine the underlying mechanism responsible for creating the paradoxical outcomes and the resulting ensemble state characteristics in the different red regimes, we use two sets of parameters $\mathcal{p}_1 = (p_1, p_2) = (0.012, 0.912)$ and $\mathcal{p}_2 = (p_1, p_2) = (0.862, 0.354)$ for purposes of illustration. We define the average probability ξ for which Branch 1 of the game is played as

$$\xi = \sum_{k=0}^{511} \frac{\pi_k m_k}{9}, \tag{10}$$

where π_k and m_k denote the stationary probability distribution and the number of individuals playing Branch 1 when the ensemble is in state S_k, respectively. Using Eq. (10), under parameters $\mathcal{p}_1$, $\xi^B = 0.4712$ and $\xi^C = 0.4351$ are obtained for **Case B** and **Case C**, respectively. Under parameters $\mathcal{p}_2$, we obtain $\xi^B = 0.2863$ and $\xi^C = 0.2894$. The expected gain is $E = \xi\left[p_1 - (1 - p_1)\right] + (1 - \xi)\left[p_2 - (1 - p_2)\right]$, from which we find the condition for a fair game ($E = 0$) to be $\xi = 0.4577$ for $\mathcal{p}_1$ and $\xi = 0.2874$ for $\mathcal{p}_2$.

For the first set of parameters $\mathcal{p}_1$, it is noted that the probability of winning in Branch 1 is small ($p_1 = 0.012$), and it is therefore an unfavorable branch. We contrast the average probabilities for playing Branch 1 in a fair game (ξ), in **Case B** (ξ^B), and in **Case C** (ξ^C), finding $\xi^B > \xi > \xi^C$. In other words, the probability of playing the unfavorable Branch 1 is higher

in **Case B** than in a fair game, but lower in **Case C** than in a fair game, explaining why $E^B < 0 < E^C$, as indeed observed in our theoretical results. For the second set of parameters p_2, Branch 1 is instead favorable due to the high winning probability ($p_1 = 0.862$), and the comparison of Branch 1 probabilities yields $\xi^B < \xi < \xi^C$, reflecting that the probability of playing the favorable Branch 1 is lower in **Case B** than in a fair case, and is higher in **Case C** than fair. This explains the $E^B < 0 < E^C$ paradoxical result observed.

Through the above analysis, we conclude that the evolution of network structure in **Case A** perturbs the neighborhood of individuals in the group, in what can be interpreted as a diffusive agitation of the game states. As a result of this, when **Case B** is selected to occur at certain time steps, the probability of playing the unfavorable branch reduces (or equivalently, the probability of playing the favorable branch increases), to produce a ratcheting effect on the game outcomes. This is analogous to the agitation-ratcheting mechanism underlying Parrondo's games. Over time, the counter-intuitive phenomenon of winning under **Case C** emerges from this mechanism.

4.2 Steady-state distribution characteristics

We divide the stationary probability distribution of the ensemble $\boldsymbol{\pi} = \{\pi_0, \pi_1, \ldots, \pi_{511}\}$ into 10 categories, each category containing states with a distinct number $h \in \{0, 1, \ldots, 9\}$ of winners. For instance, states S_1, S_2, S_4, S_8, S_{16}, S_{32}, S_{64}, S_{128} and S_{256} all belong to category 1 as they all contain only a single winner, and the distribution probability of category 1 is thus $\varpi_1 = \pi_1+\pi_2+\pi_4+\pi_8+\pi_{16}+\pi_{32}+\pi_{64}+\pi_{128}+\pi_{256}$. By analogy, we obtain the distribution probability in these 10 categories when the system evolves into steady state, as shown in Fig. 3.

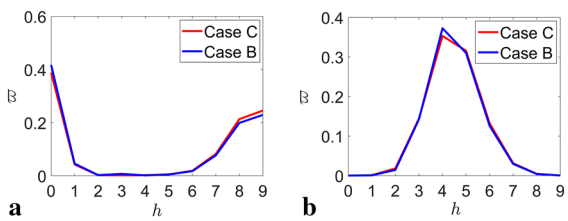

Fig. 3 Distribution probabilities for the various outcome categories in steady state, under **a** the first set of parameters p_1 and **b** the second set of parameters p_2

It is observed that under the first set of parameters p_1, the distribution characteristic of the system is concave against h. The probability of having an all-lose ($h = 0$) or all-win ($h = 9$) steady-state outcome is relatively high, in comparison with all other possible alternatives. Under the second set of parameters p_2, the distribution characteristic of the system is convex against h. The probability of having a mixed win–lose scenario, in particular categories 4 and 5, is higher than other possible alternatives.

The reason for the emergence of these two distinct distribution characteristics is that, under p_1, the probability of losing is very high ($1 - p_1 = 0.988$) when the number of winners in the neighborhood is less than the number of losers and Branch 1 is played. On the other hand, when the number of winners in the neighborhood is not less than the number of losers, Branch 2 is played, and the probability of winning is very high ($p_2 = 0.912$). Winning or losing in the current game round strongly influences the branch individuals will play in subsequent rounds of the game. For instance, when an individual wins in the current round of the game, the probability of playing Branch 2 increases in the following rounds for his neighbors. Due to the large probability of winning in Branch 2, the neighbor is likely to subsequently win, thus forming a phenomenon in which the entire group of individuals exhibits closely matched state changes, resulting in the prominence of all-lose and all-win scenarios as observed. On the other hand, under p_2, the probability of winning is high in Branch 1 ($p_1 = 0.862$), and the probability of losing is high in Branch 2 ($1 - p_2 = 0.646$). In these circumstances, a neighbor with a losing state is conducive for subsequent wins by the individual, whereas neighbors that are currently winning are detrimental in effect to the individual, as they increase the probability that the individual will play the unfavorable Branch 2. This leads to an essentially divisive phenomenon, in which individuals that win will continue to win, and vice versa for their losing counterparts. This leads to the prominence of mixed win–lose scenarios.

The above analysis suggests that there is a different win–lose assortativity in the spatial distributions of the two systems, corresponding to the two parameter sets. In the first set of parameters p_1, the win–lose assortativity between neighboring individuals appears very high, and closely matched states are observed between indi-

viduals. In the second set of parameters $\mathcal{p}_2$, win–lose relationship between neighboring individuals appears to be of higher disassortativity, ultimately culminating in the blended spatial characteristics between winning and losing states of individuals. To verify this, we establish an index ζ reflecting win–lose assortativity, defined as

$$\zeta = \sum_{k=0}^{511} \pi_k \mu_k, \tag{11}$$

$$\mu_k = \frac{1}{36} \sum_{i=1}^{9} \sum_{j=1}^{4} \left(\delta_{s_i s_j}\right)_k, \tag{12}$$

where $\left(\delta_{s_i s_j}\right)_k$ is the Kronecker delta between states s_i and $s_j \in \eta_i$ under ensemble state S_k. We obtain $\zeta^B = 0.9016$ and $\zeta^B = 0.4114$ for parameter sets $\mathcal{p}_1$ and $\mathcal{p}_2$, confirming higher win–lose assortativity and higher win–lose disassortativity, respectively.

4.3 Absorbing states of the system

It is notable that absorbing states emerge in the system for two sets of parameters, $\mathcal{p}_1^* = (p_1, p_2) = (0, 1)$ and $\mathcal{p}_2^* = (p_1, p_2) = (1, 0)$. Under parameters $\mathcal{p}_1^*$, it can be found that the **Case B** transition probability matrix $\mathbf{P}^B$ is not full rank, with rank $r = 504 < 512$. There are therefore 8 absorbing states, namely S_0, S_7, S_{56}, S_{73}, S_{146}, S_{292}, S_{448} and S_{511}, illustrated in Fig. 4. The system must evolve toward one of these states if **Case B** is always chosen at each round, and the steady-state configuration of the system must match one of these ensemble states. At the same time, we also observe that the **Case C** transition probability matrix $\mathbf{P}^C$ is not full rank, with rank $r = 510 < 512$, indicating the presence of two absorbing states. Through the agitation effects of **Case A**, the network can be excited out of the absorbing states S_7, S_{56}, S_{73}, S_{146}, S_{292} and S_{448}, but states S_0 and S_{511} remain absorbing, as these configurations are homogeneous and the states of all neighbors are left unchanged through the swapping mechanism of **Case A**.

With parameters $\mathcal{p}_2^*$, the rank of transition probability matrix $\mathbf{P}^B$ is $r = 497 < 512$, suggesting 15 absorbing states, namely S_{78}, S_{84}, S_{98}, S_{113}, S_{140}, S_{149}, S_{161}, S_{170}, S_{228}, S_{266}, S_{273}, S_{284}, S_{291}, S_{338} and S_{393}, shown in Fig. 5. It can, in contrast, be observed that $\mathbf{P}^C$ has full rank with a deterministic stationary distribution. Therefore, the agitation effects of **Case A** enable the network to jump out of all **Case B** absorbing states, leading to an absorption-free **Case C**.

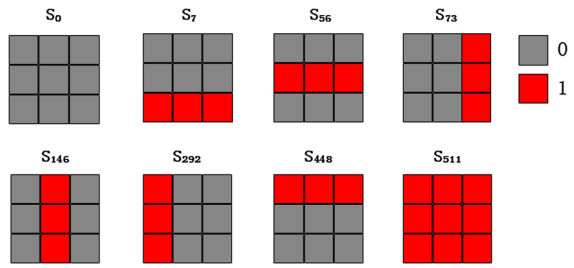

Fig. 4 Absorbing states of the system under parameters $\mathcal{p}_1^*$

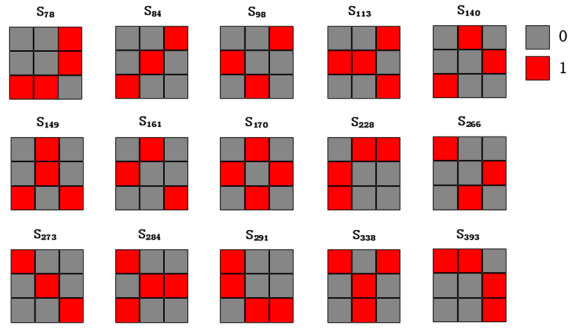

Fig. 5 Absorbing states of the system under parameters $\mathcal{p}_2^*$

In fact, the high win–lose assortativity when p_1 is small and p_2 is large (Sect. 4.2) can be observed visually in Fig. 4, and the low assortativity when p_1 is large and p_2 is small can be observed in Fig. 5. In the former, large contiguous regions of homogeneous states emerge, but in the latter winning and losing individuals are dispersed.

5 Conclusion

In the real world, neighboring niches may have both favorable and unfavorable effects on biological life, as an inexorable result of resource scarcity, competition in reproduction, and territorial expansion and defense. We had therefore developed the pure games, played in **Case B**, to have two branches. The favorable or unfavorable effects of the neighboring niches are implemented in this game structure by setting the win–lose probabilities of these two branches, and the selection between branches is dependent on the states of neighboring niches. This construction had revealed ratcheting effects of neighboring niches on the evolution of the network state, reflecting in an idealized sense biological evolution in real-world ecosystems.

Moreover, even when **Case B** was set to be losing and **Case A**, representing an evolution of the network by swapping individuals in the network, was by nature fair, alternating between **Cases A** and **B** in a random order can lead to unexpected winning outcomes with positive expected gains. A Parrondo-paradoxical phenomenon of "lose + lose = win" has thus emerged in this simplistic cell automaton system. Theoretical analysis has revealed two distinct regions in parameter space that exhibit such paradoxical results, with two corresponding ratcheting mechanisms at play. In the parameter regime of small p_1 and large p_2, a synergistic positive-feedback mechanism between an individual and its neighbors results in closely matched states, with a high degree of win–lose assortativity, and a steady-state distribution that is likely all-win or all-lose. In this regime, the ratcheting effects promote the formation of social patterns, with emergent cooperative-like phenomenon modifying fitness at a group level. On the other hand, in the second parameter regime of large p_1 and small p_2, antagonistic effects between an individual and its neighbor result in a mode of influence that is in effect divisive and exploitative, leading to mixed win–lose states and a high degree of disassortativity between individuals. In this regime, fitness is modified at the individual level and intra-group divergence is essentially uncontrolled, potentially presenting a route for the evolution of solitary lifestyles in which individuals or populations isolate themselves from counterparts exhibiting similar characteristics.

We further remark on the potential connections between the cellular automaton-based game model in this study and eco-evolutionary processes in the real world. A particularly relevant example is that of penguins, which are typical social animals. In the harsh Antarctic weather, penguins depend on inter-cooperative colony life to withstand the severe cold [34, 35]. The close clustering of penguins allows the sharing and conservation of body heat to achieve an all-win situation, similar to the phenomenon observed in Branch 2 within the first paradoxical regime (Sect. 4.2)—the greater the number of warm individuals in the neighborhood, the more likely they are to stay warm. At the same time, the harsh cold means that the temperature of penguins in the outer layers will inevitably drop, and static packing may also result in overly warm conditions for those in the interior; this temperature difference is detrimental to survival. Therefore, individual penguins regularly switch positions within their group to alternate between braving the cold at the exterior fronts and conserving heat in the interior—this is similar to the agitation effect of **Case A**. Such behavioral strategies enable improved population fitness. As a second set of examples, we consider solitary organisms, such as the cricket, mantis and scorpion [36,37]. There is strong competition between individuals in proximity to one another, resulting in prominent survival-of-the-fittest selection pressure where a divide between the strong and weak emerges and persists, similar to the second paradoxical regime; in some cases, weak individuals facing competitive disadvantage may find alternative habitats, in similar vein to the agitation of **Case A**.

Acknowledgements This project was supported by the National Natural Science Foundation of China (Grant No.11705002); Ministry of Education, Humanities and Social Sciences research projects (15YJCZH210; 19YJAZH098). KHC and JMK were supported by the SUTD Start-up Research Grant (SRG SCI 2019 142).

Compliance with ethical standards

Conflicts of interest The authors declare that they have no conflict of interest.

Appendices

Appendix A: Sample calculations for Case A

Here, we illustrate the calculation of transition probability $p_{15\to 15}$ representing a transition from state S_{15} to S_{15} ($S_{t+1} = S_t$) as shown in Fig. 1d. The ensemble remains unchanged ($S_{t+1} = S_t$) after evolution with a probability of $p_{15\to 15} = \left(C_5^2 + C_4^2\right)/C_9^2 = 16/36$.

On the other hand, for the $S_{t+1} \neq S_t$ case, taking S_{256} as an example, S_{t+1} can be one of $C_8^1 C_1^1 = 8$ different states, namely S_k with $k \in \{1, 2, 4, 8, 16, 32, 128\}$. The transition probabilities of S_{256} evolving into any of these 8 possible states are all $1/36$.

Appendix B: Sample calculations for Case B

Again, we use S_{15} (shown in Fig. 1d) as a demonstrative example when the ensemble remains unchanged ($S_{t+1} = S_t$). The states of all individuals do not change. Starting with individual 1 with a state of $s_1 = 0$, the corresponding neighbor states are $\eta_1 = \{1, 0, 0, 0\}$, and

since the number of winners is less than that of losers, Branch 1 is played with probability of winning p_1 and probability of losing $1 - p_1$. Therefore, individual 1 remains in state 0 with probability $p(1) = 1 - p_1$. In similar fashion, the probabilities for individuals 2 to 5 to remain in state 0 are $p(2) = 1 - p_1$ and $p(3) = p(4) = p(5) = 1 - p_2$, and the probabilities for individuals 6 to 9 to remain in state 1 are $p(6) = p_1$ and $p(7) = p(8) = p(9) = p_2$. This is expressed succinctly in Eq. (3). A transition probability $p_{15\to15} = (5 - p_1)/9$ is then obtained from Eq. (2).

Next, we demonstrate calculations for $p_{15\to14}$, representing the case of transition from state S_{15} to S_{14} ($S_{t+1} \neq S_t$), illustrated in Fig. 1d. Individual 9 changes from the winning state 1 to the losing state 0. The corresponding states of its four neighbors are $\eta_i = \{1, 1, 0, 1\}$. The number of winners is greater than that of losers; thus, Branch 2 of the game is played with probability of wining p_2 and probability of losing $1 - p_2$. The probability of changing from the original winning state to a losing state is therefore $\bar{p}(9) = 1 - p_2$, and the transition probability is computed to be $p_{15\to14} = (1 - p_2)/9$, as expressed in Eqs. (4) and (5).

References

1. Gardner, M.: Mathematical games: the fantastic combinations of John Conway's new solitaire game 'life. Sci. Am. **223**, 120–123 (1970)
2. Berlekamp, E., Conway, J., Guy, R.: Winning Ways for Your Mathematical Plays, Vol. 2: Games in Particular. Academic Press, New York (1982)
3. Bosch, R.A.: Maximum density stable patterns in variants of Conway's game of Life. Oper. Res. Lett. **27**(1), 7–11 (2000)
4. Tkachenko, A., Rabin, Y.: Effect of Boundary Conditions on Fluctuations and. Phys. Rev. E **7463**(1), 7146–7150 (1997)
5. Nordfalk, J., Alstrøm, P.: Phase transitions near the 'game of Life. Phys. Rev. E **54**(2), R1025–R1028 (1996)
6. Monetti, R.A., Albano, E.V.: Critical edge between frozen extinction and chaotic life. Phys. Rev. E **52**(6), 5825–5831 (1995)
7. Bak, P., Chen, K., Creutz, M.: Self-organized criticality in the Game of Life. Nature **342**(6251), 780–782 (1989)
8. Jin, W., Chen, F.: Topological chaos of universal elementary cellular automata rule. Nonlinear Dyn. **63**(1), 217–222 (2011)
9. Souyah, A., Faraoun, K.M.: An image encryption scheme combining chaos-memory cellular automata and weighted histogram. Nonlinear Dyn. **86**(1), 639–653 (2016)
10. Souyah, A., Faraoun, K.M.: Fast and efficient randomized encryption scheme for digital images based on Quadtree decomposition and reversible memory cellular automata. Nonlinear Dyn. **84**(2), 715–732 (2016)
11. Wang, X., Xu, D.: A novel image encryption scheme using chaos and Langton's Ant cellular automaton. Nonlinear Dyn. **79**(4), 2449–2456 (2015)
12. Toral, R.: Cooperative Parrondo's games. Fluct. Noise Lett. **1**(01), L7–L12 (2001)
13. Mihailović, Z., Rajković, M.: One dimensional asynchronous cooperative Parrondo's games. Fluct. Noise Lett. **3**(04), L389–L398 (2003)
14. Ethier, S.N., Lee, J.: Parrondo games with spatial dependence and a related spin system, II. Markov Process. Relat. Fields **19**(4), 667–692 (2013)
15. Mihailović, Z., Rajković, M.: Cooperative Parrondo's games on a two-dimensional lattice. Phys. A Stat. Mech. Appl. **365**(1), 244–251 (2006)
16. Ethier, S.N., Lee, J.: Parrondo games with two-dimensional spatial dependence. Fluct. Noise Lett. **16**(01), 1750005 (2017)
17. Parrondo, J.M.R., Harmer, G.P., Abbott, D.: New paradoxical games based on Brownian ratchets. Phys. Rev. Lett. **85**(24), 5226–5229 (2000)
18. Harmer, G.P., Abbott, D.: A review of Parrondo's paradox. Fluct. Noise Lett. **02**, R71–R107 (2002)
19. Abbott, D.: Asymmetry and disorder: a decade of parrondo's paradox. Fluct. Noise Lett. **09**(01), 129–156 (2010)
20. Abbott, D., Harmer, G.P.: Game theory: losing strategies can win by Parrondo's paradox. Nature **402**(6764), 864–864 (1999)
21. Soo, W.W.M., Cheong, K.H.: Parrondo's paradox and complementary Parrondo processes. Phys. A Stat. Mech. Appl. **392**(1), 17–26 (2013)
22. Soo, W.W.M., Cheong, K.H.: Occurrence of complementary processes in Parrondo's paradox. Phys. A Stat. Mech. Appl. **412**, 180–185 (2014)
23. Cheong, K.H., Soo, W.W.M.: Construction of novel stochastic matrices for analysis of Parrondo's paradox. Phys. A Stat. Mech. Appl. **392**(20), 4727–4738 (2013)
24. Cheong, K.H., Koh, J.M., Jones, M.C.: Paradoxical survival: examining the Parrondo effect across biology. BioEssays **41**(6), 1900027 (2019)
25. Toral, R.: Capital redistribution brings wealth by Parrondo's paradox. Fluct. Noise Lett. **2**(04), L305–L311 (2002)
26. Ye, Y., Xie, N.-G., Wang, L.-G., Meng, R., Cen, Y.-W.: Study of biotic evolutionary mechanisms based on the multiagent parrondo's games. Fluct. Noise Lett. **11**(02), 1250012 (2012)
27. Szolnoki, A., Perc, M.: Information sharing promotes prosocial behaviour. New J. Phys. **15**(5), 53010 (2013)
28. Cheong, K.H., Koh, J.M., Jones, M.C.: Multicellular survival as a consequence of Parrondo's paradox. Proc. Natl. Acad. Sci. **115**(23), E5258–E5259 (2018)
29. Koh, J.M., Xie, N., Cheong, K.H.: Nomadic-colonial switching with stochastic noise: subsidence-recovery cycles and long-term growth. Nonlinear Dyn. **94**(2), 1467–1477 (2018)
30. Koh, J.M., Cheong, K.H.: Automated electron-optical system optimization through switching Levenberg–Marquardt algorithms. J. Electron Spectros. Relat. Phenomena **227**, 31–39 (2018)

31. Koh, J.M., Cheong, K.H.: New doubly-anomalous Parrondo's games suggest emergent sustainability and inequality. Nonlinear Dyn. **96**, 257–266 (2019)
32. Cheong, K.H., Koh, J.M., Jones, M.C.: Do arctic hares play Parrondo's games? Fluct. Noise Lett. **18**(03), 1971001 (2019)
33. Wu, D., Szeto, K.Y.: Extended Parrondo's game and Brownian ratchets: strong and weak Parrondo effect. Phys. Rev. E **89**(2), 22142 (2014)
34. Gilbert, C., Robertson, G., Le Maho, Y., Naito, Y., Ancel, A.: Huddling behavior in emperor penguins: dynamics of huddling. Physiol. Behav. **88**(4–5), 479–488 (2006)
35. Ancel, A., Beaulieu, M., Le Maho, Y., Gilbert, C.: Emperor penguin mates: keeping together in the crowd. Proc. R. Soc. B Biol. Sci. **276**(1665), 2163–2169 (2009)
36. Ahsan, M.M., Tahir, H.M., Mukhtar, M.K., Ali, A., Kahan, Z.I., Ahmed, K.: Intra-and inter-specific foraging in three scorpion species. Punjab Univ. J. Zool. **31**(1), 69–76 (2016)
37. Huntingford, F.A.: Animal Conflict. Springer, Berlin (2013)

Publisher's Note Springer Nature remains neutral with regard to jurisdictional claims in published maps and institutional affiliations.